

Nanoheterostructures And Nanoheterojunctions Based on ZnO/ZnSe for Nanomedicine

Received: 18 October 2022, **Revised:** 24 November 2022, **Accepted:** 26 December 2022

Dilnoza Baxtiyorovna Elmurotova

1PhD., Associate Professor, Department of "Biomedical Engineering" Tashkent State Technical University, Islam Karimov, 100095, Tashkent, University St., 2. *e-mail: elmurotova.tdtu@mail.ru, dilnoza_elmurodova@mail.ru

Malika Anvarovna Mussayeva

2DSc., Professor, Institute of Nuclear Physics AS RUz, pos. Ulugbek, 100214, Tashkent, Uzbekistan *e-mail: mussaeva@inp.uz

Gulnoza Saydullayevna Uzoqova

3 Associate Professor, Department of "General Physics" Karshi State University, 180119, Karshi city, Kuchabag street, house-17

Zilola Maxsudjon qizi Raximberganova

1assistant, Department of "Biomedical Engineering" Tashkent State Technical University, Islam Karimov, 100095, Tashkent, University St., 2.

Farxod Quvondiqovich Shakarov

1senior lecturer, Department of "Biomedical Engineering" Tashkent State Technical University, Islam Karimov, 100095, Tashkent, University St., 2.

Nodiraxon Saidvoris qizi Yusupova

1assistant, Department of "Biomedical Engineering" Tashkent State Technical University, Islam Karimov, 100095, Tashkent, University St., 2.

Keywords:

nanoheterojunction, nanoheterostructure, photovoltage-current characteristic, optical absorption, electroluminescence

Abstract

The high-resistance n-type ZnSe/ZnO:O nanoheterostructure after doping with Te and heat treatment in an oxidizing medium had p-n-nanoheterojunctions due to the generation of Frenkel pairs. This led to the formation of two induced resonant levels $\Gamma_{6v} - 5.76$ eV and $L_{1,3v} - 4.85$ eV is also shown in the optical absorption spectra, with the formation of a semiconductor structure and electroluminescence at $\lambda_{max}=600$ nm.

Of particular interest in this aspect are quantum dots (QD). QD have characteristic sizes from a few to 100 nm, in which a significant fraction of atoms (about 1% [1]) is located on the surface of nanoparticles (NP), as a result, they have an increased reactivity and add (donate) atoms of the environment.

Quantum dots are nanosized crystals of spherical or elliptical shape in the form of nanorods and nanoshells, as well as in the form of "nanorods", "nanostars", or "nanocells" structures [2-4]. The spatial limitation of the motion of charge carriers in QD leads to a quantum-

size effect, which is expressed in the discrete structure of electronic levels. When light photons hit QD, a plasmon resonance (PR) can arise in them due to the excitation of localized surface plasmon polaritons (SPP) at the interface between the media. To reduce the toxicity of QD, they are covered, for example, with polymer shell, which can enhance PR. There can be several shells, and as a result, several interfaces between the media that enhance the PR appear.

In terms of luminous intensity, the best QD are those that have the highest quantum yield and fluorescence

time. The advantage of QD over other fluorophores lies in their unique optical properties: high photostability and quantum yield, wide spectrum of absorption frequencies, the possibility of tuning a narrow spectrum of emission frequencies, and the purity of possible luminescence colors.

The most important characteristics of QD include the spectrum of absorption (QD is an acceptor, A) and emission (QD is a donor, D) of light. These QD characteristics significantly depend on the chemical composition of the core and shells, the ratio of their diameters at given wavelength of incident light. At present, large amount of research has been carried out in which various aspects related to the use of nanoparticles (microchips, MEMS technologies, the transition to quasi zero dimensional (0D) nanostructures — quantum dots and quantum rings), nanobiotechnologies (biosensorics, genomics, visualization, photothermolysis of cancer cells, targeted delivery of drugs, enhancement of the immune response, anti-infective properties, etc.) for the creation of solar cells and photodetectors [3, 4].

The results obtained became the basis for the active use of QD in various fields of nanomedicine for diagnostic and therapeutic purposes [3]. It was also found that for the effective use of QD in biomedicine, it is necessary that NP resonances in the optical range fall within the “transparency window” of biological tissues [5].

Based on the foregoing, **the goal of this work** was to study the effect of ZnO growth on the electrooptical properties of ZnSe.

1. Characteristics of objects and research methods:

Objects: We studied ZnSe crystals grown at the Monocrystal Research Institute, Kharkov [6] in a reducing medium with an impurity of 0.2 wt.% Te. The samples were thermally treated in zinc vapor to reduce nonradiative surface recombination and increase conductivity. At the same time, the Zn/Se ratio increased, that is, nonstoichiometricity.

Research methods: Measurements of the optical density spectra (D) were carried out on an SF-56A (LOMO) spectral instrument equipped with a computer program for recording and processing the obtained spectra in the wavelength range from 190 to 1100 nm

at 300 K. Table 1 presents the optical densities (OD) in absorption band maxima and their corresponding transition energies; stable energy resonance levels (RL) are marked with an asterisk. Levels and transitions were identified in accordance with theoretical calculations of the band structure of pure ZnSe, taking into account the temperature in the sequence: $A_{1,3c}$, Γ_{6v} , $L_{1,3}$, M_{4v} etc. [7]. The concentration of optical centers N (cm^{-3}) responsible for the isolated absorption band was calculated using the Smakula formula [8]:

$$N = 1.28 \cdot 10^{17} \frac{n}{(n^2 + 2)^2} \cdot \frac{K_m H}{f}; \quad (1)$$

where n -is the refractive index for the wavelength corresponding to the absorption band maximum, in the case of E_g -the bands for the ZnSe crystal $n=2.6645$; f - the strength of the oscillator for transitions involving the zone is equal to 1; H -is the half-width of the band, (eV); K_m - absorption coefficient at the band maximum (cm^{-1}); is the electron concentration at the E_g level.

- Current-voltage dependences were measured by two-contact method with indium contacts on standard devices at 300 K in the dark and under illumination with an incandescent lamp (continuous emission spectrum). The brightness of the incandescent lamp was measured with a Guarda FX-101 LUX METER and was 2280 Lumens.

- Measurements of the electroluminescence (EL) spectra and volt-radiance characteristics (VRC) were carried out on the SPM-2 spectral instrument, in the wavelength range of 200-900 nm at 300 K. A constant voltage was applied from the power supply in the forward and reverse directions. First, a low voltage of both polarities was applied, the EL spectrum was taken, and the band maximum was determined. The threshold voltage was determined by the beginning of the appearance of EL

According to X-ray fluorescence analysis, the samples in the near-surface layer were non-stoichiometric and contained 1% excess of zinc [9]. The initial superstoichiometry of Zn in the near-surface layer is due to the volatility of selenium and increases after heat treatment in zinc vapor. We have also shown that ZnSe/ZnO:O nanoheterostructure (NHS) has a size of ZnO nanocrystalites up to 27 nm, and ZnSe(0.2Te)/ZnO:O,Zn nanoheterojunction (NHJ) up to 40 nm.

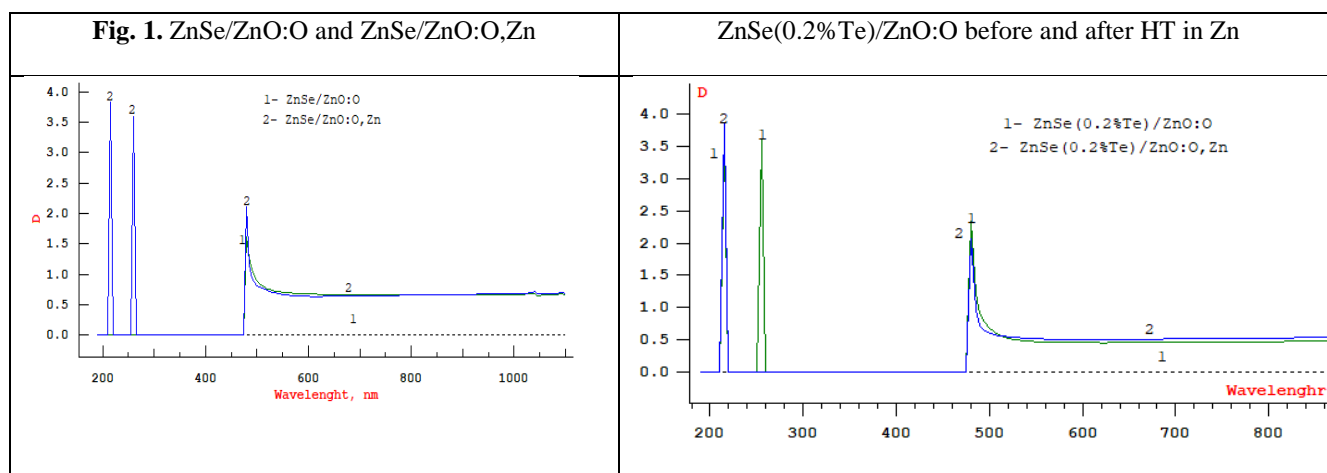


Table 1. Energies (eV) and OD (D) of RI and calculations of N_e in NHS ZnSe/ZnO:O and NHJ ZnSe(Te)/ZnO:O,Zn

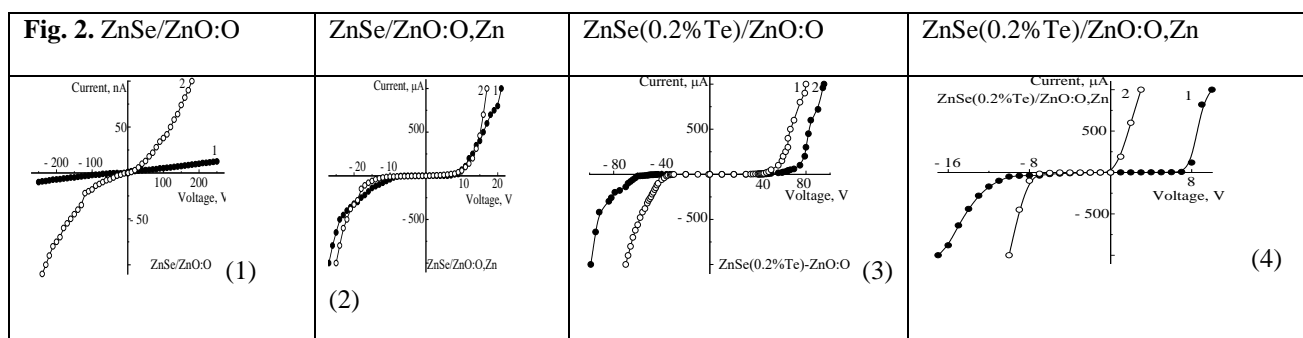
NHS ZnSe/ZnO:O	NHJ ZnSe/ZnO:O,Zn	NHJ ZnSe(0.2%Te)/ZnO:O	NHJ ZnSe(0.2%Te)/ZnO:O,Zn
	Γ_{6v} -5.76 eV-3.84 $N_{\Gamma_{6v}}=2.63 \cdot 10^{16} \text{ cm}^{-3}$	Γ_{6v} -5.76 eV -3.54 $N_{\Gamma_{6v}}=2.25 \cdot 10^{16} \text{ cm}^{-3}$	Γ_{6v} -5.76 eV -3.84 $N_{\Gamma_{6v}}=2.44 \cdot 10^{16} \text{ cm}^{-3}$
	$L_{1,3v}$ -4.76 eV -3.6 $N_{L_{1,3v}}=1.77 \cdot 10^{16} \text{ cm}^{-3}$	$L_{1,3v}$ -4.85 eV -3.6 $N_{L_{1,3v}}=1.65 \cdot 10^{16} \text{ cm}^{-3}$	-
$E_g=2.58 \text{ eV} -1.62$ $N_{E_g}=1.26 \cdot 10^{16} \text{ cm}^{-3}$	$E_g=2.58 \text{ eV} -2.11$ $N_{E_g}=0.43 \cdot 10^{16} \text{ cm}^{-3}$	$E_g=2.58 \text{ eV} -2.33$ $N_{E_g}=0.5 \cdot 10^{16} \text{ cm}^{-3}$	$E_g=2.58 \text{ eV} -2.07$ $N_{E_g}=0.34 \cdot 10^{16} \text{ cm}^{-3}$
$N_e=1.26 \cdot 10^{16} \text{ cm}^{-3}$	$N_e=4.83 \cdot 10^{16} \text{ cm}^{-3}$	$N_e=4.38 \cdot 10^{16} \text{ cm}^{-3}$	$N_e=2.78 \cdot 10^{16} \text{ cm}^{-3}$

Here are the results of experimental studies of the OP spectra of NHS ZnSe/ZnO:O (cr. 1), NHJ ZnSe/ZnO:O,Zn (cr. 2) and ZnSe(0.2%Te)/ZnO:O (cr. 1), ZnSe (0.2%Te)/ZnO:O,Zn (cr. 2), as well as calculations of the electron density (N_e) using the Smakula formula (Table 1). All obtained curves are reproducible with an error in $\Delta\lambda=1 \text{ nm}$. From fig. 1 on the right - it can be seen that in the NHS ZnSe/ZnO:O with a thickness of 27 nm, the maximum D reached up to 1.62, at $E_g=2.58 \text{ eV}$ (480 nm) with $N_e=1.26 \cdot 10^{16} \text{ cm}^{-3}$; the formation of two RI, clearly distinguished by narrow peaks, including Γ_{6v} -5.76 eV and $L_{1,3v}$ - 4.76 eV with $N_e=4.83 \cdot 10^{16} \text{ cm}^{-3}$ and E_g - 2.58 eV with OD up to 2.11.

Also from Fig. 1 on the left, it can be seen that doping of Te with NHJ ZnSe(0.2%Te)/ZnO:O led to the formation of the Γ_{6v} and $L_{1,3v}$ RI, as well as an increase in N_e by 3.5 times, i.e. up to $4.38 \cdot 10^{16} \text{ cm}^{-3}$, when both HT in zinc vapors NHJ ZnSe(0.2%Te)/ZnO:O,Zn led to the destruction of the $L_{1,3v}$ RI with $E_g=2.58 \text{ eV}$ with N_e up to $2.8 \cdot 10^{16} \text{ cm}^{-3}$. Apparently, this is due to the diffusion of cations from the surface into the depths, and as result, the Fermi level rises, near-surface donor states are formed, which serve as sites for the growth of the thickness of ZnSe nanoclusters. The optical absorption of such 0-dimensional quantum dots is characterized by very narrow and intense resonances in the UV region of the spectrum due to the large oscillator strength and the reduction in the number of possible transitions (quantum confinement).

Table 2. - Dark (ρ_d) and light (ρ_l) resistivity, polarization (+R/-R) and photoconductivity (σ_{FC})

NHS and NHJ	ρ_d , ohm·cm	+R/-R	ρ_l , ohm·cm	+R/-R	σ_{FC} , ohm ⁻¹
NHS ZnSe/ZnO:O	+4.8·10 ⁹	0.87	+1.1·10 ⁹	0.81	+0.71·10 ⁻¹⁰
	-5.5·10 ⁹		-1.35·10 ⁹		-0.56·10 ⁻¹⁰
NGJ ZnSe/ZnO:O,Zn	+4.6·10 ⁵	0.11	+1.83·10 ⁵	0.52	+0.33·10 ⁻⁶
	-41·10 ⁵		-3.5·10 ⁵		-0.28·10 ⁻⁶
NGJ ZnSe (0.2%Te)/ZnO:O	+6.9·10 ⁸	0.25	+1.4·10 ⁸	0.2	+0.6·10 ⁻⁹
	-2.7·10 ⁹		-7.1·10 ⁸		-0.1·10 ⁻⁹
NGJ ZnSe (0.2%Te)/ZnO:O,Zn	+2.3·10 ⁵	0.07	+2.2·10 ⁵	0.08	+0.02·10 ⁻⁶
	-3.1·10 ⁶		-2.8·10 ⁶		-0.03·10 ⁻⁷



In table 2. shows the calculated data for dark resistivity ρ_d and light resistivity ρ_l , as well as the corresponding values of polarization (+R/-R) and σ_{FC} for NHS ZnSe/ZnO:O with high ρ values, low σ_{FC} values and high polarization in the light and in the dark, NHJ ZnSe/ZnO:O,Zn, i.e. heat treatment in Zn vapor, led to a decrease in ρ_d and ρ_l by 4 orders of magnitude, as well as to a decrease in polarization, with an increase in σ_{FC} by 4 orders of magnitude, due to formation of Frenkel pairs.

It can also be seen that the doping of NHS ZnSe/ZnO:O to 0.2%Te led to an order of magnitude decrease in ρ_d and ρ_l depending on the polarity and polarization, with an increase in σ_{FC} by an order of magnitude, where subsequent HT in NHJ ZnSe(0.2%Te)/ZnO:O,Zn led to a decrease in ρ_d and ρ_l by 3 orders of magnitude, as well as to a significant decrease in polarization and an

increase in σ_{FC} by 2 orders of magnitude, depending on the polarity.

On fig. 2 shows the photo-voltage characteristics of high-resistance NHS ZnSe/ZnO:O, which had a linear pattern in the dark; ohmic CVC, where a photo-sensitive semiconductor structure (SCS) was formed in the light at high voltages. As a result of HT in Zn vapor and doping with an isovalent impurity in NHJ, a PBL formed due to the formation of deep, stable, electrically active centers, which explains the decrease in ρ by 4 orders of magnitude, which persists even in the presence of light. The slopes of the I-V characteristics, characteristic of the SCS, above the cutoff voltage, determine the collisional ionization processes according to the law $I=KU^\beta$.

NHS ZnSe/ZnO:O with current-conducting In contacts had an ohmic photo-voltage characteristic and no EL was formed on them. According to literature data, it is

known that in wide-gap ZnSe crystals, after doping with Te and TO impurity in Zn vapor, luminescence is excited thermally-TL, X-ray photo-PL with a maximum at 580 nm, 600 nm, 620 nm, that is, a recombination level is created in band gap with

different Stokes shifts of radiative transitions [6]. The surface layer of ZnO plays the role of an injection contact on the p-ZnSe layer, as well as a “window” for outputting radiation. Below are the spectra of the VRC, EL of the studied NGJ at reverse and direct polarity.

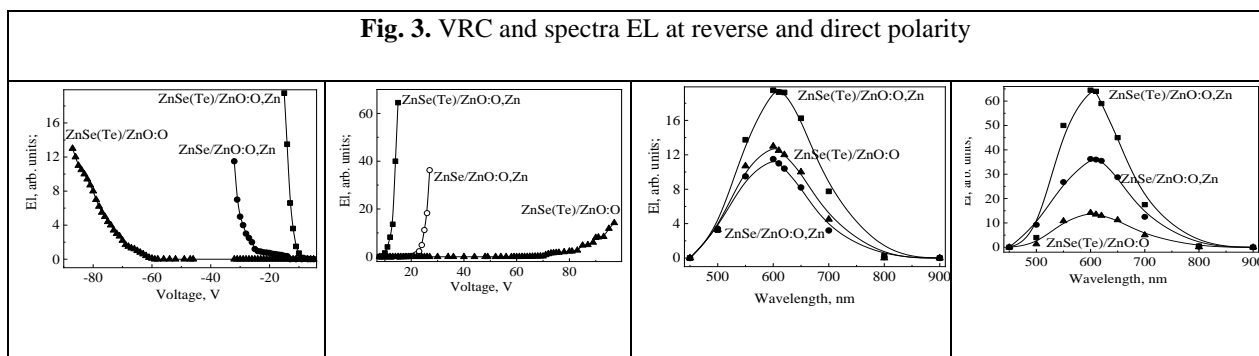


Fig. 3 shows the VRC and EL spectra of the indicated NHJ at $\lambda_{\max}=600$ nm ($Zn_i=2.06$ eV). It can be seen that the NHJ ZnSe/ZnO:O,Zn appears EL when applying $U>\pm 12$ V, depending on the polarity $I_{EL}=11.5$ at ($U=-32$ V) and $I_{EL}=36.3$ at ($U=27$ V). It is known that the low intensity of the orange glow can be associated either with a low Zn_i concentration or with the absence of the ZnO nanophase even at high O impurity concentration in ZnSe [10].

A characteristic group of narrow absorption bands at 7.1, 6.8, 6.5, 6.2, and 5.8 μm in the IR transmission spectra was attributed to multiple ZnO precipitates in the ZnSe volume, which appear during cooling of the condensate or during aging. Therefore, the increase in EL can be explained by an increase in the nonequilibrium concentration of Frenkel pairs and e-h pairs, some of which were localized on defects such as Zn_i and ZnO precipitates. Frenkel pairs are formed in NHJ after HT in an oxidizing medium and Zn vapor, doping with Te, when a semiconductor and light-emitting structure is formed. Doping of the NHJ ZnSe/ZnO:O with an isovalent impurity Te formed SCS in the NHJ ZnSe(0.2%Te)/ZnO:O at high voltages, as shown in Fig. 2; $U>\pm 60$ V, EL appears, while the samples were very hot, which led to degradation of the electrodes, where, depending on the polarity, the EL intensity (I_{EL}) reached 13 at ($U=-87$ V) and $I_{EL}=14$ at ($U=97$ V).

Upon doping with an isovalent Te impurity, stable, low-mobility associates $V_{Zn}+Te$ are formed in ZnSe crystals; subsequent HT in an O medium and in Zn

vapor form more highly mobile radiative centers Zn_i and stable associates $V_{Zn}Te_{Se}Zn_i$ [6-10]. HT in Zn vapors NHJ ZnSe(0.2%Te)-ZnO:O,Zn leads to a significant decrease in the blocking voltage, when, as the excitation voltage of the EL at $\lambda_{\max}=600$ nm, it decreased to $U>\pm 6$ V by 10 times, the dependence on polarity increased $I_{EL}=19.5$ and 64.5 at $U=\pm 15$ V (Fig. 3).

In our case, the intensity of yellow-orange EL ($\lambda_{\max}=600$ nm) depended on the presence of the Te impurity, where in ZnSe/ZnO:O,Zn NHJ $I_{EL}=36$, and in ZnSe(0.2%Te)/ZnO:O,Zn $I_{EL}=65$ with thin ZnO film. The resulting n-ZnO surface layer plays the role of an injection contact to the p-ZnSe(Te)/n-ZnO:O,Zn layer, and this material can be recommended for use as an LED in the yellow-orange region of the spectrum, which is natural for human eyes.

2. Conclusions:

It has been shown that in high-resistance n-type ZnSe/ZnO:O samples after doping with Te and heat treatment in an oxidizing medium, p-n-nanoheterojunctions are formed due to the generation of Frenkel pairs in both sublattices and electron-hole pairs and the recharging of centers. In the optical absorption spectra in the mode of strongly absorbing objects, two induced resonance levels $\Gamma_{6v} - 5.76$ eV and $L_{1,3v} - 4.85$ eV were determined, it was also found that the HHJ ZnSe/ZnO:Zn, ZnSe(0.2%Te)/ZnO:O and ZnSe(0.2%Te)/ZnO:O,Zn with a semiconductor structure have light-emitting properties in the range of

Journal of Coastal Life Medicine

450–900 nm, due to an increase in the concentration of stable associates $V_{Zn}Te_{Se}Zn_i$.

The authors are grateful to V. D. Ryzhikov for the presented samples of zinc selenide.

The research was carried out with financial support from the Scientific Researches Program to President Degree 4526 of 21.11.2019.

Reference

- [1] V.O. Ponomarev at all. Evaluation of the Ophthalmotoxic Effect of Quantum Dots InP/ZnSe/ZnS 660 and Bioconjugates Based on Them in Terms of the Prospects for the Treatment of Resistant Endophthalmitis // *Ophthalmology in Russia*, 2021;18(4):876–884. <https://doi.org/10.18008/1816-5095-2021-4-876-884>
- [2] D.B. Elmurotova at all. Amplification of photoconductivity of ZnSe/ZnO:O nanoheterostructures after reactor irradiation // *Euroasian Journal of Semiconductors Science and Engineering*. V.2 Is. 5, A13. 10-24-2020. P. 55–59.
- [3] A.I. Galanov at all. Development of magnetic nanostructured iron-based materials as potential vectors for drug-delivery application. *Siberian oncological journal*. 2008;3(27):50–57.
- [4] N.G. Khlebtsov at all. Optics and biophotonics of nanoparticles with a plasmon resonance // *Quantum Electronics*. 2008;38(6):504–529.
- [5] V.A. Oleinikov at all. Fluorescent Semiconductor Nanocrystals in Biology and Medicine // *Russian nanotechnologies*. 2007;2(1–2):160–173.
- [6] B.V. Grinyov at all. Scintillation detectors and systems of radiation monitoring on their base // *Ukrainian scientific book in a foreign language*, Kyiv, 2010, P.342.
- [7] T.V. Gorkavenko at all. Temperature dependence of the band structure of wurtzite type semiconductor compounds: ZnS, ZnSe, ZnTe, CdTe // *Semiconductors*, 2007. V.41. N8. P.908–916.
- [8] B.V. Budylin, A.A. Vorobyov. Effect of radiation on ionic structures // *Moscow*. 1962. Ch. 2. P.38.
- [9] A. A. Kist, N. M. Mukhamedshina, E. M. Ibragimova. *Czechoslovak Journal of Physics*, v. 52, Suppl. A, P. A21 (2002).
- [10] N.K. Morozova. Role of background O and Cu impurities in the optics of ZnSe crystals in the context of the band anticrossing model // *Semiconductors*, 2008. V.42. N2. P.131–135.